International Symposium
on :
Utilization of underground space in urban areas
6-7 November 2006, Sharm El-Sheikh, Egypt

RATIONAL ANALYSIS OF TUNNELS SUBJECTED TO DIFFERENT EXPLOSIEVE LOADS

Dr. ADEL MAHMOUD BELAL
Assistant Prof. of Civil Engineering Military Technical College, Cairo, Egypt

ABSTRACT

Due to the progressive development of military destructive weapons such as conventional weapons, a consequence development of the fortified structures is essential. One of the most important types of the fortified structures is tunnel in rock media. A numerical simulation of ground shock from detonations in rock is extremely demanding, requiring hydrodynamic computer codes, combined with non-linear dynamic codes based on discrete elements, discrete fracture and finite elements, which is a very complex approach.

The basic premise of this work is studying the response of tunnels in rock-media exposed to high explosion loads, which help the designers and military engineers in estimating displacements, stresses and over all damage in the tunnels due to wave propagation generated by that explosion loads. The numerical analysis is carried out using finite element technique, the commercial software package, AUTODYN; version 4.3 was used to perform three-dimensional nonlinear dynamic analysis used in this study. This program is probably the most extensive code dealing with explosive loads in the world.

This paper, gives an overview of simpler approach, based on the use statistically treated of the finite element results with physical principles and analytical solutions to idealized cases. This approach mostly ends up in easy to use closed form prediction equations, which thus constitute a rational tool for practical solution of commonly encountered ground shock problem. In this study, simple equations are developed for different responses of rock tunnel in different parameters based on a regression analysis of the results of a 72 3D-F.E. models.

Key Words: Finite Element, Under Ground, Explosion Wave, Rock Soil, Tunnel.

1- FINITE ELEMENT VALIDATION

One of the most important problems in modeling dynamic non-linear problem is the performance of the used material model in handling the non-linear behavior of the rock under failure conditions. However, the elastic-plastic material model for rock is generally accepted to model the non-linear behavior. There are a large variety of models, which have been proposed in recent years to characterize the stress-strain and failure behavior of rock media. The common relatively simple material models with yield surface are Von Mises [13], Mohr-Coulomb [5] Johnson-Holmquist [7], and RHT models [11]. The performance of the four material models in characterizing the stress-strain and failure behavior of rock media has been investigated for a field test with available measurements. A comparison between AUTODYN finite element models results and the field test measurements is performed for the four material models.

1.1 Description of the Field Test Problem

The selected problem to be investigated is a field-blasting test carried out at the granite site by Zohu [15]. The field layout, as shown in Fig. 1, consists of a step charge hole with a total depth of 11m. The upper 6m of the charge hole has a diameter of 1.5m and the bottom 5 m has a diameter of 0.8m. The measuring point was placed at 25m distance from the charge hole center. The test is carried out with an equivalent TNT charge weight 50 kg.

1.2 Axial Symmetric Finite Element Calibration Model

The finite element program AUTODYN is used to create finite element models for the previous field test problem [15] using the above four material models. The used finite element mesh is shown in Fig. 2. A brief description of the modeling procedures for different parts of the problem is presented as follows:

1.2.1 .Air and TNT

The numerical modeling, air and equivalent explosive TNT are simulated by 200 elements Euler processor mesh and are assumed to satisfy the equation of state EQS of ideal gas and EQS of JWL respectively, second form is known as the “Jones - Wilkins - Lee” (JWL) equation of state, standard constant of air and TNT are from the AUTODYN.

1.2.2 Rock and concrete

Rock and concrete are simulated by 3040 elements of Lagrange processor as illustrated in Fig. 2, Transmitting boundary is used to reduce reflection of stress wave from the numerical boundaries. The material constants of the rock mass obtained from site investigation are used in the numerical simulation. These include Poisson’s ratio of the granite ν=0.16; averaged mass density of granite 2650 kg/m^3; the elastic modulus of undamaged rock material is estimated to be 93.87Gpa; average uniaxial compressive strength is 175Mpa, average tensile strength is 17.5Mpa where the equivalent critical tensile strain ε_{cr}=0.000275. Concrete standard constants are used in the concrete model.
Four strength models are used in this study, and general comparison between different material models is illustrated in Table 1, such as arrival time, peak particle acceleration and frequency. Fig. 3, Fig. 4 and Fig.5 Fig.6 shows the field result acceleration and the computed acceleration time history by using Von Mises, Mohr-Coulomb, Johnson-Holmquist, and RHT material models respectively, at target point (25m from the detonation).

From table 1 and from Fig.3 to Fig. 6, it is clear that, RHT-material model has the perfect match with field results in terms of arrival time, peak amplitudes and frequency.

1.3 Three-Dimensional Finite Element Calibration Model

In order to verify the result obtained by the axial-symmetry F.E. model, a three-dimensional F.E. model is created for the same field test problem by using RHT material model. A quarter of the problem was modeled for symmetry as shown in Fig.7. The same boundary condition and load case were applied to this model. The acceleration-time history at the same target point of the axial-symmetric model is shown in Fig.8, where the result has a good agreement with the field-measured data.

3 FINITE ELEMENT ANALYSIS

The general view for vertical side wall tunnel is shown in figure (9). Since the problem is symmetric about the X, Y-axes and for saving time, only a quarter of the domain is taken as the computation model. The model dimensions in the X, Y-axes are 5R and 7.5m respectively. The non-reflection boundary is given by transmitting the boundary conditions at ambient rock masses, the plan X=0 and Y=0 are treated as symmetric boundary.

Material properties for poor, moderate and hard rock, adopted in these models are shown in table (1). The values of strength and moduli are determined from numerous references [3] , and [6]. The rock is assumed to be continuous, isotropic and homogeneous medium. RHT brittle material model is used for characterizing the nonlinear behavior of the rock.

In order to demonstrate the effect of tunnel radius (R) on the response of tunnel, three spans are used; 3m, 4.5m, and 6m. Also, the effect of crown-detonation distance (D) is studied by using three distances between charge and tunnel crown; 10m, 15m and 20m as shown in figure (9).

For all cases, an explosion of 2500 kg of TNT at 3.25m-distance bellow ground surface is applied. Three points, crown, spring and invert point are used to study the displacement and internal forces. Table (3) shows the general response for twenty seven cases.

The tunnel span 9m is used to investigate the charge effect with the different rock properties and different crown detonation distances where the charge weight varies from 0 to 2500 kg TNT, the tunnel response for these cases are shown in table (4).

4- NONLINEAR REGERATION

The commercial software Data Fit [2] is used to determine the best-fit parameters for a model by minimizing a chosen merit function. The process is to start with some initial estimates and incorporates algorithms to improve the estimates iteratively. The new estimates then become a starting point for the next iteration. These iterations continue until the merit function effectively stops decreasing. Displacements analysis and plastic strain are performed, while stresses and displacement of steel lining are performed. The following symbols are used in the predicted equations:

δ_{crown} : Peak displacement at tunnel crown (cm)
δ_{spring} : Peak displacement at spring (cm)
δ_{invert} : Peak displacement at invert (cm)
δ_{f} : Failure displacement at tunnel crown (cm)
ε_{crown} : Peak strain at tunnel crown
t_s : Steel lining thickness (cm)
t_c : Concrete lining thickness (cm)
σ_{max} : Maximum stress in steel lining (MPa)
E :Modulus of elasticity of rock (GPa)
Q :Charge weight (kg)
D_f :The failure crown-detonation distance (m)
R : The tunnel radius for circular section or half span for VSW tunnel (m)

4.1 For the 2500kg TNT Charge Weight

Based on finite element results in table (2), the predicted equations for tunnel without lining are accomplished as in table (5), these equations can be used only for 2500 kg TNT.
The predicted equation of peak plastic strain at tunnel crown is shown in the following equation

$$\varepsilon_{crown} = 2.8\frac{e^{0.14.R}}{e^{0.377D+0.056E}}$$

4.2 Charge Effect and General Equation

The responses for 45 case of VSW tunnel under different charge weights from 0 to 2500 kg TNT are shown in table (4). Based on these results, the predicted equations for tunnel without lining are accomplished as in table (6), these equations can be used for any charge weight from 0 to 2500 kg TNT.
The predicted equation of peak plastic strain at tunnel crown is shown in the following equation:

$$\varepsilon_{crown} = 2.8 \frac{e^{0.14.R}}{e^{0.377D+0.056E}} \left(\frac{Q}{2500}\right)^{1.178}$$

5- CONCOLUSION

From this study, simple equations are developed. These equations show a good agreement with the results of the finite element complicated models. Designers can use these equations in the preliminary study for different tunnel projects in rock media.

REFERENCES

[1] **AUTODYN 2003**, computer finite element program
[2] **DataFit**, computer statistical program, 2005.
[3] **Fred G. B.** , "Engineering Properties of Soil and Rock", Department of Geology and Applied Geology, University of Natal, Durbon, South Africa, Blackwell science, 2000.
[4] **Ma, G.W., H.Hao & Y.X.Zhou** "Modeling of Wave Propagation Induced by Underground Explosion" Computer and Geotechnics, Vol. 22,No. ¾, pp. 283- 303, 1998
[5] **Hoek V D**,(1978). " Modeling of concrete by a Mohr-coulomb model", PISCES Tech. Note TN-7803, Physics International, December 1978
[6] **Jemes F**., "Tunneling Technology", the Ontario of transportation and communication, 1976.
[7] **Johnson G. R. & Holmquist T. J.** (1993). An Improved Computational Constitutive Model for Brittle Materials, Joint AIRA/APS Conference, Colorado Springs, Colorado, June 1993.
[8] **Johnson, G R, & Cook, W H** (1983). "A Constitutive Model and Data for Metals Subjected to Large Strains, High Strain Rates and High Temperatures", Proc. Seventh Int. Nat.Symposium on Ballistics, April 1983
[9] **Otis Williams** (1997) "Engineering and Design Tunnels and Shafts in Rock"Washington
[10] **Riedel W**., "Impact and Explosion RHT. Model", PhD Thesis, EMI report no. 6/00, Freiburg, Germany, July, 2000.
[11] **Riedel W.,Thoma K., Hiermaier S**. (1999) and Schmolinke, E., Penetration of Reinforced Concrete by Beta-B-5000 Numerical Analysis Using a New Macroscopic Concrete Model for Hydrocodes, Proceedings of the 9th International Symposium on the Effects of Munitions with Structures, Berlin-Straussberg, Germany
[12] **TrueGrid** Mesh Generator, computer program, 2003.
[13] **Von Mises, R** (1928). Z.Angew Math. u. Mech.,8, [English Translation: UCRL Trans. 872]
[14] **Wiliams o**., "Engineering Design of Tunnels and Shafts in Rock", CECW-ED, department of the army US.Army corps of engineers, 1997.
[15] **Zhou Y.,** (2000) "Numerical analysis of blast-induced stress wave in anisotropic rock mass with continuum damage models" Nanyang Technological University,2000
[16] **Hussein Lolo, A. M. Belal, I. M. Kamal, M. Mohmedein**, " Finite Element Analysis of Tunnels" PhD Thesis, Military Technical College, Cairo, Egypt, 2005

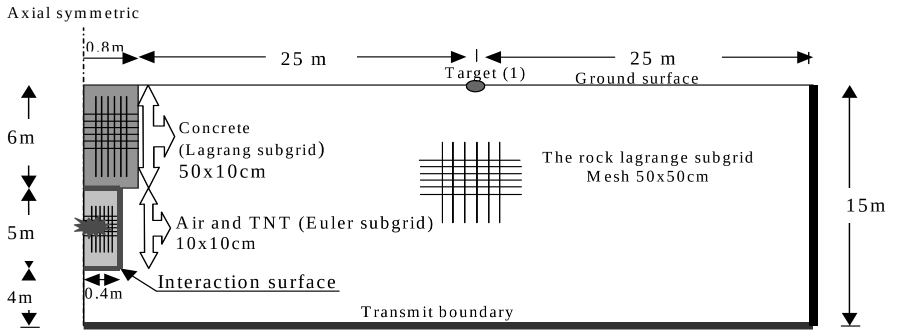

Fig. 1 Layout of Test

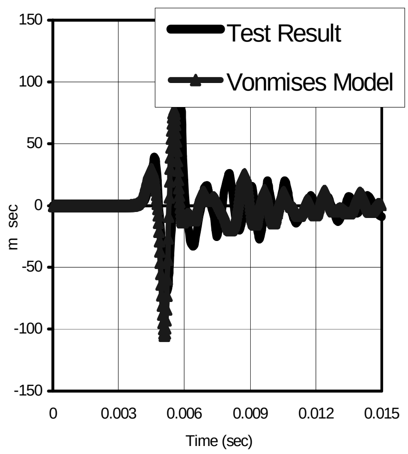

Fig. 3 Test versus FE
(Von Mises model response)

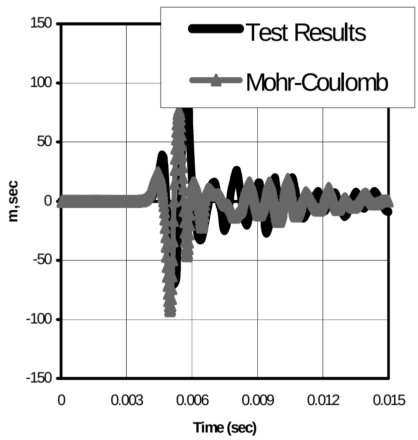

Fig. 4 Test versus FE
(Mohr-Coulomb model response)

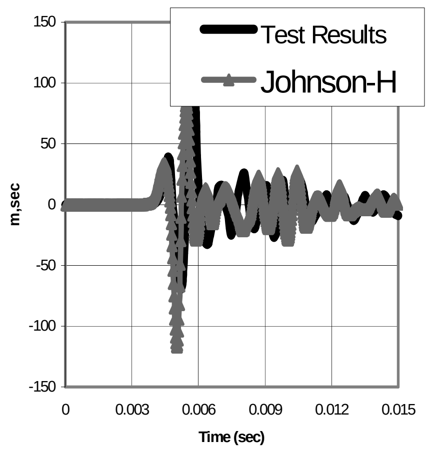

Fig. 5 Test versus FE
(Johnson-Holmquist model response)

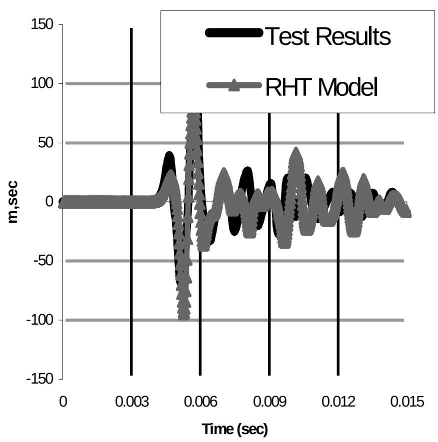

Fig. 6 Test versus F.E.
(RHT model response)

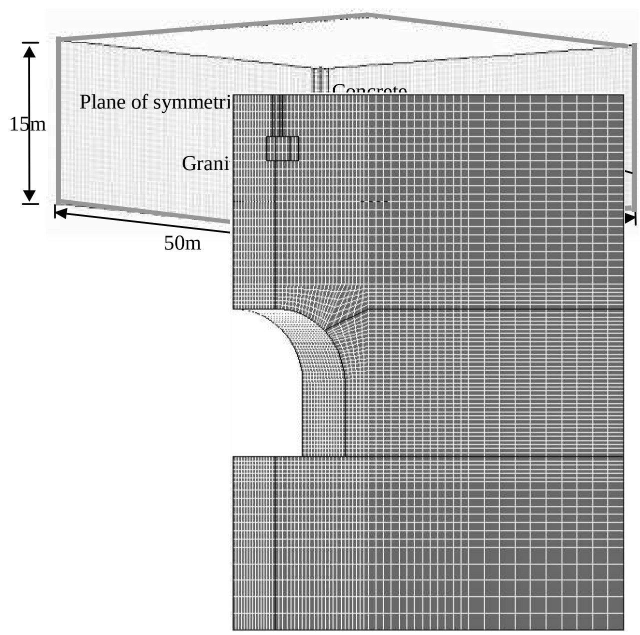

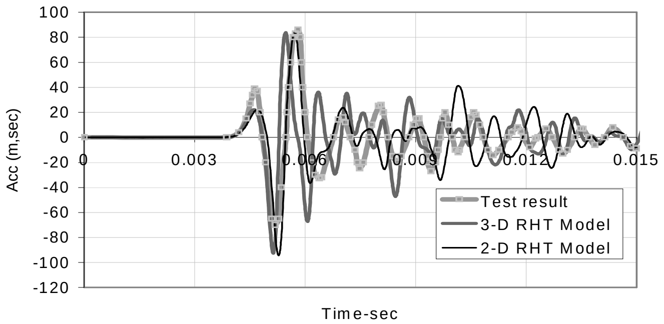

Fig. 8 Test versus finite element F.E, 2-D and 3-D.
with RHT model response

Fig. (9) ATOUDYN-3D FE mesh

Table (1) %Matching of finite element responses with material models and field measurements

Geometry model	Material Model	Comparison %			
		Arrival time	Peak Amplitude (PPA)		Frequency
			Negative	Positive	
Axial Of sym. Model	Von Mises	95	150	89	118
	Mohr-Coulomb	95	132	89	100
	Johnson-Holmquist	95	167	97	100
	RHT	95	134	98	109
3-DMODEL	**RHT**	95	133	97	118

Table (2) Rock properties

Rock Type	**Rock Quality Design (RQD) %**	**Rock Mass Ratting (RMR) %**	**Density γ t/m³**	**Modulus of elasticity E Gpa**	**Poisson ratio ν**	**Bulk Modulus K Gpa**	**Shear Modulus G Gpa**	**Unc. Com. Strength Mpa**	**Failure Strain**
Hard	90	85	2.75	70	0.23	43.21	28.45	100	0.0025
Mod.	50-75	65	2.4	30	0.25	20	12	25	0.005
Poor	25-50	44	2.21	8.5	0.3	7.083	3.27	10	0.0075

Table (5) The displacement predicted equations at crown, spring and invert for 2500 kg TNT

Table (6) The general displacement predicted equations at crown, spring and invert

Displacements (cm)	Standard Error (cm)	Error %
$\delta_{crown} = 18.14 . e^{\frac{30}{D}} . \frac{R^{0.8}}{D} . \frac{1}{(0.3E+0.9)^{1.4}} (\frac{Q}{2500})^{1.614}$	0.2	12.4
$\delta_{spring} = 5.97 \frac{1}{e^{0.0051D+0.331R+0.036E}} (\frac{Q}{2500})^{1.135}$	0.05	11.3
$\delta_{H-spring} = 1.377 \frac{e^{0.119R}}{e^{0.1D+0.02E}} (\frac{Q}{2500})^{0.8}$	0.049	16
$\delta_{invert} = 5.06 \frac{e^{0.0126D}}{e^{0.45R+0.028E}} (\frac{Q}{2500})^{0.97}$	0.053	12.6

locations	The predicted equations	Standard error (cm)	Deviation %
Vertical displacement at crown (cm)	$\delta_{crown} = 18.14 . e^{\frac{30}{D}} . \frac{R^{0.8}}{D} \frac{1}{(0.3E+0.9)^{1.4}}$	0.497	12.12
Vertical displacement at spring (cm)	$\delta_{spring} = 5.97 \frac{1}{e^{0.0051D+0.331R+0.036E}}$	0.137	19.6
Horizontal displacement at spring (cm)	$\delta_{H-spring} = 1.35 \frac{e^{0.119R}}{e^{0.1D+0.02E}}$	0.063	22.6
Vertical displacement at invert (cm)	$\delta_{invert} = 5.08 \frac{e^{0.0126D}}{e^{0.45R+0.028E}}$	0.098	25.3

Table (3) Peak response of VSW tunnel under 2500kg TNT explosive

Span (m)	D(m)	Rock	PPD Vertical (cm)			PPA Vertical (m/s^2)			PPD.H .(cm)	PPA.H (m/s^2)	Ref.
			CRW.	SPR.	INV.	CRW.	SPRI.	INV.	SPR.	SPR.	
	10	Poor	13.8	1.71	1.3	5669	4623	690	0.65	3532	V3P10
		Moderate	3.01	0.523	0.53	8872	5618	1864	0.405	1817	V3M10
		Hard	0.94	0.41	0.273	14260	6114	3231	0.253	1844	V3H10
	15	Poor	3.73	1.49	1.3	3445	3150	559	0.33	2205	V3P15
		Moderate	1.03	0.55	0.56	5998	3669	1542	0.215	2262	C3M15
		Hard	0.41	0.43	0.38	12090	3540	2142	0.062	1096	V3H15
		Poor	2.33	1.45	1.3	2704	2183	605	0.123	1544	V3P20

		Moderate	0.79	0.612	0.614	5734	2490	1100	0.066	845	C3M20
		Hard	0.42	0.423	0.43	7547	3119	1349	0.035	842	V3H20
9	10	Poor	22.3	0.91	0.58	5949	3605	522	0.7	2652	V4P10
		Moderate	4.1	0.25	0.18	9075	4160	1139	0.46	1493	V4M10
		Hard	1.6	0.088	0.04	14930	4514	1983	0.3	1703	V4H10
	15	Poor	5.29	0.94	0.68	3753	2560	556	0.48	1828	V4P15
		Moderate	1.21	0.35	0.33	6414	2822	869	0.285	1254	V4M15
		Hard	0.3	0.247	0.266	11300	3730	1412	0.077	874	V4H15
	20	Poor	2.66	0.95	0.765	2875	1808	500	0.31	1393	V4P20
		Moderate	0.664	0.355	0.357	4969	1861	777	0.12	1092	V4M20
		Hard	0.285	0.275	0.277	7074	2459	1066	0.054	698	V4H20
12	10	Poor	29.4	0.61	0.311	5802	2527	374	0.824	1703	V6P10
		Moderate	5.4	0.19	0.093	7351	3185	737	0.456	1139	V6M10
		Hard	2.17	0.07	0.027	16180	3394	1591	0.36	1463	V6H10
	15	Poor	6.92	0.584	0.32	3884	2337	358	0.633	1459	V6P15
		Moderate	1.45	0.19	0.088	6816	2361	740	0.294	1069	V6M15
		Hard	0.285	0.146	0.138	11460	3103	954	0.079	835	V6H15
	20	Poor	3.23	0.615	0.39	3086	1502	405	0.41	1205	V6P20
		Moderate	0.706	0.226	0.192	4696	1590	757	0.165	833	V6M20
		Hard	0.21	0.157	0.148	7033	1835	819	0.058	775	V6H20

Table (4) Response of VSW tunnel under different charge weights

Mod-el	E (Gpa)	D (m)	Q (kg)	p-	P+	δ_{crown}	δ_{spring}	δ_{invert}	$\delta_{H-spring}$	$\varepsilon_{p-crown}$	$\varepsilon_{p-crown}/\varepsilon_{f}$
1	8.5	10	0	0	0	0	0	0	0	0	0
2	8.5	10	417	-2.49	0.784	1	0.111	0.08	0.136	0.00295	0.393
3	8.5	10	833	-2.5	1.27	3.822	0.261	0.15	0.36	0.01616	2.154
4	8.5	10	1250	-2.435	1.69	7.13	0.416	0.281	0.55	0.04	5.333
5	8.5	10	1667	-1.96	2	11	0.582	0.4	0.656	0.055	7.333
6	8.5	10	2500	-2.6	2.4	22.3	0.91	0.58	0.7	0.075	10
7	8.5	15	0	0	0	0	0	0	0	0	0
8	8.5	15	417	-1.322	0.612	0.343	0.116	0.012	0.09	0.000151	0.020
9	8.5	15	833	-1.853	1.15	1.02	0.236	0.23	0.19	0.00203	0.270
10	8.5	15	1250	-2.016	1.041	1.991	0.45	0.355	0.311	0.00378	0.504
11	8.5	15	1667	-1.996	1.107	2.984	0.63	0.472	0.381	0.00553	0.737
12	8.5	15	2500	-2.1	1.04	5.29	0.94	0.68	0.48	0.01133	1.510

13	8.5	20	0	0	0	0	0	0	0	0	0
14	8.5	20	417	-0.746	1.02	0.24	0.14	0.167	0.1	0.000025	0.003
15	8.5	20	833	-1.15	1.176	0.607	0.281	0.22	0.123	0.000192	0.025
16	8.5	20	1250	-1.467	1.353	1.1	0.466	0.465	0.177	0.000717	0.095
17	8.5	20	1667	-1.736	1.7	1.603	0.624	0.57	0.221	0.00106	0.141
18	8.5	20	2500	-1.8	2.78	2.66	0.95	0.765	0.31	0.00144	0.192
19	30	10	0	0		0	0	0	0	0	0
20	30	10	417	-3.8	0.632	0.161	0.031	0.024	0.032	0.000122	0.024
21	30	10	833	-4.96	1.64	0.508	0.06	0.04	0.08	0.00142	0.284
22	30	10	1250	-4.7	2.74	1.19	0.097	0.05	0.24	0.00376	0.752
23	30	10	1667	-4.96	1.5	1.95	0.135	0.12	0.35	0.01337	2.674
24	30	10	2500	-5.5	1.88	4.1	0.25	0.18	0.46	0.022	4.4
25	30	15	0	0	0	0	0	0	0	0	0
26	30	15	417	-1.97	1.04	0.081	0.054	0.055	0.0246	0.0000012	0.00024
27	30	15	833	-3.13	1.82	0.208	0.123	0.124	0.054	0.000126	0.0252
28	30	15	1250	-4.07	1.87	0.39	0.14	0.15	0.0977	0.000625	0.125
29	30	15	1667	-4.683	1.82	0.6	0.181	0.19	0.133	0.0015	0.3
30	30	15	2500	-4.43	2.34	1.21	0.29	0.25	0.285	0.002	0.4
31	30	20	0	0	0	0	0	0	0	0	0
32	30	20	417	-1.01	1.15	0.04	0.1	0.08	0.0036	0	0
33	30	20	833	-1.76	2.19	0.165	0.134	0.123	0.058	0.000015	0.003
34	30	20	1250	-2.4	2.84	0.276	0.2	0.2	0.0791	0.000412	0.0824
35	30	20	1667	-2.8	3	0.375	0.233	0.251	0.091	0.00015	0.03
36	30	20	2500	3.62	3.43	0.664	0.355	0.357	0.12	0.00055	0.11
37	70	10	0	0	0	0	0	0	0	0	0
38	70	10	417	-4.833	1.31	0.052	0.015	0.02	0.0161	0	0
39	70	10	833	-8.33	0.876	0.12	0.03	0.032	0.029	0.00002	0.008
40	70	10	1250	-11	1.28	0.254	0.117	0.118	0.05	0.000164	0.0656
41	70	10	1667	-12.9	2.186	0.967	0.0656	0.059	0.22	0.006	2.4
42	70	10	2500	-14	7.72	1.6	0.088	0.04	0.3	0.00783	3.132
43	70	15	0	0	0	0	0	0	0	0	0
44	70	15	417	-2.52	2.09	0.032	0.0136	0.016	0.0076	0	0
45	70	15	833	-4.3	3.74	0.064	0.047	0.047	0.0248	0	0
46	70	15	1250	-6	3.77	0.124	0.1164	0.118	0.0355	0	0
47	70	15	1667	-7.42	4.16	0.175	0.155	0.158	0.05	0.000024	0.0096
48	70	15	2500	-9.63	4.47	0.3	0.155	0.266	0.077	0.00021	0.084
49	70	20	0	0	0	0	0	0	0	0	0
50	70	20	417	-1.21	1.4	0.0228	0.01662	0.018	0.0095	0	0
51	70	20	833	-2.57	2.42	0.0512	0.0536	0.056	0.024	0	0
52	70	20	1250	-3.8	4.1	0.136	0.14	0.142	0.031	0	0
53	70	20	1667	-4.5	5	0.2	0.1	0.1	0.04	0.00001	0.005
54	70	20	2500	-5.95	6.5	0.29	0.09	0.08	0.05	0.0000275	0.011